

# Numerical prediction of the foam structure of polymeric materials by direct 3D simulation of their expansion by chemical reaction based on a multidomain method

J. BIKARD\*, J. BRUCHON, T. COUPEZ, B. VERGNES

*Centre de Mise en Forme des Matériaux (CEMEF), Ecole des Mines de Paris, UMR CNRS 7635, BP 207, 06904, Sophia Antipolis, France*  
E-mail: [jerome.bikard@ensmp.fr](mailto:jerome.bikard@ensmp.fr)

The quality of thermosetting polymer foams (like polyurethane foam, used for example in automotive industry) mainly depends on the manufacturing process. At a mesoscopic scale, the foam can be modelled by the expansion of gas bubbles in a polymer matrix with evolutionary rheological behaviour. The initial bubbles correspond to germs, which are supposed quasi-homogeneously distributed in the polymer. An elementary foam volume ( $\sim 1 \text{ mm}^3$ ) is phenomenologically modelled by a diphasic medium (polymer and immiscible gas bubbles). The evolution of each component is governed by equations resulting from thermodynamics of irreversible processes: the relevant state variables in gas, resulting from chemical reaction creating carbon dioxide (assimilated then to a perfect gas), are pressure, temperature and conversion rate of the reaction. The number of gas moles in each bubble depends on this conversion rate. The foam is considered as a shear-thinning viscous fluid, whose rheological parameters evolve with the curing reaction, depending on the process conditions (temperature, pressure). A mixed finite element method with multidomain approach is developed to simulate the average growth rate of the foam during its manufacture and to characterize the influence of the manufacturing conditions (or initial rheological behaviour of the components) on macroscopic parameters of the foam (cell size, heterogeneity of porosity, wall thickness).

© 2005 Springer Science + Business Media, Inc.

## 1. Introduction

The economic challenges related to industry require a better knowledge of the phenomena taking a significant place during the manufacturing processes of polymeric foams, which are more and more present in automotive and aeronautic applications. For example, flexible polyurethane (PU) foams are today used in many industrial parts. These PU foams are produced in a one-shot process, in which polyisocyanate, resin and water are mixed simultaneously with suitable stabilisers, catalysts and cell-size control agents. The chemical reactions begin immediately in this liquid medium, with foam rise starting a few seconds after mixing and being completed in a matter of minutes, producing polyurea and carbon dioxide [1, 2], with simultaneous expansion of  $\text{CO}_2$  bubbles (foaming due to blowing agents) and polymerization of the mixture. The latter, obtained at high pressure, is then injected into the mold. After a first step of germination ( $\text{CO}_2$  molecules, dissolved in the mixture, are concentrated in micro-bubbles, due to

pressure evolution), the bubbles are nourished in gas by production of  $\text{CO}_2$  due to a first chemical reaction. A second reaction governs the cure of the matrix (the walls between the gas bubbles). Both reactions are exothermic.

Taking into account these phenomena and their consequences is essential to better control the process and to produce high quality final products. The optimization of the manufacturing process, as well as final product quality, may be improved through numerical modelling. Two ways can be considered. At a macroscopic scale, a phenomenological model has been proposed to describe the evolving rheological properties of the mixture during the manufacturing process [3–5]. At a microscopic scale, the interactions between gas bubbles and liquid walls can be studied (expansion, coalescence). The aim of the numerical model presented in this paper is to allow the simulation of the growth and the coalescence of gas bubbles within a polymer matrix, which simulates in the present case

\*Author to whom all correspondence should be addressed.

the expansion of a foam by chemical reactions. It gives to the polymer a close or an open cells foam texture [3], which will be simultaneously stabilised by the curing reaction, conferring to the foam its final characteristics. The present paper briefly presents the framework of the model (based on the thermodynamics of irreversible processes of diphasic mediums) and proposes numerical applications with finite element method.

**2. State variables and constitutive equations**

At the macroscopic scale, the liquid mixture appears as a quasi-homogeneous continuous medium. Its rheological main characteristics are viscoplasticity or viscoelasticity [4, 5]. But, at a microscopic scale, the material behaviour depends on the interactions between all reactants, and also on the conditions of moisture, pressure and temperature during the process [4]. The bubbles grow in this mixture. The microscopic material domain considered in this study corresponds to an elementary representative volume of foam during its expansion. We suppose that this volume can be defined and is representative of the macroscopic material at each step of the manufacturing process. The microscopic material domain can then be assimilated to a medium constituted by two phases: the first is the viscous polymer, whose rheological properties evolve during the process due to the curing reaction; the second is the gas, resulting from a second chemical reaction, which is randomly distributed in the matrix as bubbles.

At first approximation, the matrix is considered as a shear-thinning fluid whose rheological parameters depend on the degree of curing, denoted  $\beta$  (the viscoelastic properties are neglected in this study). The gas contained in the bubbles will be modelled as a perfect gas. The number of moles  $n_i$  in the bubble  $i$  depends on the rate of creation of  $\text{CO}_2$  present in this bubble. Denoted  $\alpha_i$ , it models the chemical reaction induced by the blowing agents. The two variables  $\alpha_i$  and  $\beta$  are supposed to follow evolution laws, function of time, pressure and temperature. In a first approximation, the interfacial tension will be neglected in the model, because it weakly affects the form of the interface, in comparison with the high viscosity of the matrix. However it would have to be taken into account in the case of coalescence, i.e. when the film of fluid separating them becomes very thin.

The conservation equations (mass and momentum) are written in each phase (matrix and bubbles), as well as the general principles of thermodynamics [6]. In order to take into account the interactions between the various phases, interface laws are considered [7]. If quasi-static evolutions are supposed, we have:

$$\left\{ \begin{array}{ll} \text{div} \sigma = 0 & \text{in liquid and bubbles} \\ \sigma = \sigma_1 = 2\eta(\dot{\gamma}, T, \beta)\varepsilon(v) - pI & \text{in the liquid} \\ \sigma = \sigma_i = -p_i I \text{ with } p_i V_i = n_i(\alpha_i)RT & \text{in the bubble } i \\ \text{interface conditions} & \end{array} \right. \quad (1)$$

$\sigma$  is the Cauchy stress tensor,  $\varepsilon(v)$  the strain rate tensor,  $\dot{\gamma} = \sqrt{\varepsilon(v) : \varepsilon(v)}$  its equivalent measurement ( $:$  is the scalar product of tensors),  $p$  the local pressure in the liquid,  $\eta$  and  $p$  the viscosity and the hydrostatic pressure of the liquid.  $p_i$  is the homogeneous pressure in the bubble  $i$ ,  $V_i$  its volume,  $R$  the perfect gas constant and  $T$  the temperature. The interface conditions assume the continuity of the normal velocity and the normal stress (the interfacial tension is neglected).

The creation of gas and the curing reactions are governed by chemical kinetics, whose conversion rate is supposed to follow an evolution law, as in [1, 5]. Concerning the creation of gas, a Prime law [8] is assumed:

$$\frac{\partial \alpha_i}{\partial t} + v \cdot \nabla \alpha_i = \lambda_g S_i (1 - \alpha_i)^{\mu_g} \quad (2)$$

$\lambda_g$  is the characteristic rate of gas creation by surface unit, depending on the temperature,  $S_i$  is the surface of the wall around the bubble  $i$  (through which the dissolved  $\text{CO}_2$  is diffused) and  $\mu_g$  the exponent of this reaction. The number of moles in each bubble depends on the conversion rate  $\alpha_i$ , according to [9]:

$$n_i(\alpha_i) = n_i^0 (1 + \kappa_i \alpha_i) \quad \text{in the bubble } i \quad (3)$$

$n_i^0$  is the initial number of moles in the bubble  $i$  and  $\kappa_i$  the rate of moles created by the reaction in this bubble ( $\kappa_i = (n_i^{\text{max}} - n_i^0)/n_i^0$ ,  $n_i^{\text{max}}$  being the final number of moles in the bubble  $i$ , after reaction). Note that  $\kappa_i$  depends on the bubble, which makes heterogeneous the bubbles expansion in the fluid. Simultaneously, a second chemical reaction leads to the polymerization of the matrix, such that its viscosity increases up to the gel point. As for the gas conversion rate, an evolution reaction is considered for the curing rate, which is supposed to follow a Piloyan law [10]:

$$\frac{\partial \beta}{\partial t} + v \cdot \nabla \beta = \lambda_p \beta^{\mu_p} (1 - \beta)^{\nu_p} \quad (4)$$

$\lambda_p$  is the characteristic rate of the cure and  $\mu_p$  and  $\nu_p$  two exponents. Taking into account that the reactions are exothermic, we consider now the heat equations in the liquid and the bubbles:

$$\left\{ \begin{array}{ll} \rho c \dot{T} = k \Delta T + \dot{w} & \text{in liquid and bubbles} \\ c = c_l, k = k_l \quad \text{and} \quad \dot{w} = 2\eta(\dot{\gamma}, T, \beta)\varepsilon(v) : \varepsilon(v) + \delta H_p \dot{\beta} & \text{in the liquid} \\ c = c_v n_i, k = k_i \quad \text{and} \quad \dot{w} = -p_i \frac{\dot{V}_i}{V_i} + \delta H_g \dot{\alpha} & \text{in the bubble } i \\ \text{interface thermal conditions} & \end{array} \right. \quad (5)$$

$c$  is the heat capacity of the material,  $k$  is the heat conductivity,  $\delta H_g$  and  $\delta H_p$  respectively the enthalpy of gas creation and of curing of the matrix around the bubbles. At the interface, heat transfer by conduction and convection mechanisms is assumed.

### 3. Numerical simulation

The system governed by Equations 1–5 is highly coupled and non-linear. Thus, a splitting technique has been used to decrease the degree of complexity: on one time step, knowing  $T$ ,  $\alpha_i$  and  $\beta$ , velocity and pressure fields are determined through a mixed finite element method. The velocity is then used to compute the temperature. Finally, the velocity and the temperature are used to compute the gas production and the polymerization rate.

Furthermore, we consider that  $v$  and  $p$  are discontinuously interpolated in time. The elements of the Eulerian mesh are  $d$ -simplexes (triangles in 2D, tetrahedra in 3D), where  $d$  is the spatial dimension. In what concerns spatial discretization,  $(v, p)$  have to satisfy stability conditions: finite element approximation of the velocity and pressure have to verify the inf-sup condition [11]. In our approximation, we chose a linear interpolation for velocity and pressure with bubble enrichment for velocity, the P1+/P1 element, also referred as the MINI-element [12].

Once the velocity field is established, we have to determine the temperature. The heat balance equation is solved using a mixed formulation in temperature and heat flow. As for the mechanical problem, the finite element must verify stability conditions [13].

Once the temperature field is established, we have to calculate the gas rate and the curing rate (as well as free surface evolution). On the element, the gas rate and the curing rate are interpolated by functions that are constant and discontinuous in space, and polynomial and discontinuous in time.

Finally, in order to calculate the position of the moving interface between the gas-liquid mixture, the characteristic functions of bubbles are used as additional unknowns in each time interval [14] and solved by a finite element based volume of fluid (V.O.F.) method associated with a Space-Time Discontinuous Galerkin technique: Even though the method performs well, numerical diffusion exists and may give incorrect description of the interface. To limit this diffusion, a  $r$ -adaptation technique is used [15]. This technique is based on the displacement of mesh nodes without changing the mesh topology: the mesh follows the motions of the fluid by contracting the nodes at the interfaces, regaining its original size once the interface has passed.

The model has been implemented through the Rem3D<sup>®</sup> software (developed by CEMEF) [16].

### 4. Examples of application

#### 4.1. Case of a single bubble in an infinite medium

The model is first validated in the case of the expansion of a single bubble in a quasi-infinite Newtonian fluid, for which an analytical solution exists for Equations 1 and 2. In this case, the following assumptions are made [9]:

- the behaviour of the fluid is given by the Newton law (we note  $\eta_0$  the viscosity) and there is no curing reaction,

- the characteristic rate of the reaction  $\lambda_g$  is supposed constant,
- assuming an adiabatic fluid/bubble interface, the temperature variations in the bubble are only due to its expansion (endothermic evolution) and to the creation of gas (exothermic evolution),

Under these hypotheses, thermomechanical equations (Equation 5) are weakly coupled because the interfaces are adiabatic and the characteristic rate of the chemical reaction does not depend on the temperature. It is possible to find the explicit solution of Equations 1 and 2 by extension of the analysis carried out by Amon and Denson [7]. Denoting by  $p_{ext}$  the pressure around the quasi-infinite domain and  $p_0$  the initial pressure in the bubble, we introduce the following parameters:

$$\mu = \frac{3p_{ext}}{4\eta_0} \quad \text{and} \quad g(t) = \frac{n(t)T(t)}{n_0T_0} \quad (6)$$

A 1D balance equation leads to the bubble volume at time  $t$ :

$$V_b = V_0 \left[ e^{-\mu t} + \mu \frac{p_0}{p_{ext}} \int_0^t g(s) e^{-\mu(t-s)} ds \right]^3 \quad (7)$$

where  $V_0$  is the initial volume of the bubble (corresponding to a numerical initial condition). The pressure is independent of the initial radius and of the initial number of moles present in the bubble. The initial number of moles,  $n_0$ , satisfies the perfect gas law ( $n_0 = \frac{p_0 V_0}{RT_0}$ ). In the case of an isothermal expansion, and assuming that  $\mu_g = 1$ , the analytic solution can be explicitly written as:

$$V_b = V_0 \left[ 1 + \kappa - \frac{\kappa}{1 - \frac{4\eta_0}{3p_0} \lambda_g} \left( e^{-\lambda_g t} - \frac{4\eta_0}{3p_0} \lambda_g e^{-\frac{3p_0}{4\eta_0} t} \right) \right]^3 \quad (8)$$

The material parameters are given in Tables II at the reference temperature  $T_{ref} = 25^\circ\text{C}$ . The thermal parameters correspond to the CO<sub>2</sub> gas, but the parameters of the reaction law have been arbitrarily estimated. We assume also that  $p_0 = p_{ext} = 10^5$  Pa.

The comparison between analytical and numerical solutions is presented in Fig. 1: a good correlation between these two results is observed. Discrepancy could be explain by boundary effects. In the analytical solution, the radius evolves to a limit value. The evolution is first slow (for short times), then the curve shows an inflection point. Afterwards, a small creation of gas generates a strong increase of the radius. The study of this analytical solution in function of the material parameters shows that  $\mu$  ratio and  $\kappa$  are the main parameters.  $\mu$  is homogeneous to a deformation rate and  $\mu \frac{p_0}{p_{ext}}$  characterises the mobility of the fluid around the bubble. It represents the opposition between the pressure forces in the bubble and the viscosity forces in the liquid. The pressure is independent of the initial radius and of the initial number of moles present in the bubble. Fig. 2 shows the evolution of pressure in the bubble with time. The pressure first evolves strongly

# MECHANICAL BEHAVIOR OF CELLULAR SOLIDS

TABLE I Material parameters and variables used in the study

Variables and parameters	Name	Parameters	Name
Velocity field	$v$	Perfect gas constant	$R$
Cauchy stress tensor	$\sigma$	Density	$\rho$
Hydrostatic pressure	$p$	Viscosity	$\eta$
Strain rate tensor	$\varepsilon(v)$	Characteristic time of gas rate reaction	$\lambda_g$
Equivalent rate of deformations	$\dot{\gamma}$	Exponent of gas rate reaction	$\mu_g$
Temperature	$T$	Initial number of moles in one bubble	$n^0$
Conversion rate of gas creation	$\alpha$	Rate of moles created in one bubble	$\kappa$
Conversion rate of polymerisation	$\beta$	Characteristic time of polymerisation reaction	$\lambda_p$
Volume of one bubble	$V$	First exponent of polymerisation reaction	$\mu_p$
Surface of one bubble	$S$	Second exponent of polymerisation reaction	$\nu_p$
Number of gas moles in one bubble	$n$	Heat capacity	$c$
Time	$t$	Heat conductivity	$k$
Dissipated power	$\dot{w}$	Enthalpy of gas creation	$\delta H_g$
Reference temperature for Arrhenius law	$T_{ref}$	Enthalpy of polymerisation	$\delta H_p$
Activation energy	$E$	Atmospheric pressure	$p_{ext}$
Exponent of Carreau law	$m$	Gel point	$\beta_{gel}$
Characteristic time of Carreau Law	$a$	Gel exponent	$n_g$
Identity tensor in $R^3$	$I$	<b>Indices:</b> Relative to the liquid phase	$l$
Gradient	$\nabla$	Relative to the $i$ th bubble $i$	$i$
Laplacien	$\Delta$	Initial value 0	

in the bubble, whereas the radius evolves slowly (see Fig. 1). After a maximum (at  $t \approx 1$  s), the pressure in the bubble decreases to the atmospheric pressure, whereas its radius continues to increase. It can be explained by the behaviour of the fluid near the interface during the expansion: larger is the viscosity of the fluid, slower is the expansion. The maximum of the pressure curve corresponds to the equilibrium between the pressure in the bubble and the efforts of cohesion in the liquid. When this equilibrium is passed, the viscosity of the liquid is no more sufficient to limit the expansion of the bubble. Above  $t \approx 15$  s, it can be considered that the expansion occurs with a constant pressure.

## 4.2. 3D Simulation of the foam expansion

This simulation deals with the expansion of a representative volume of foam of  $1 \text{ mm}^3$ , in which a distribution of 8, 27, 64 or 125 small bubbles are randomly embedded. These dimensions have been chosen such that, after expansion, the expanded volume (the numeric "foam") contains a number of cells in good agreement with the real observations, with a realistic size of the cells [17]. Considering that this volume is representative of the centre of the foam (far from the skin), a constant pressure is imposed on its 6 faces (this condition is characteristic of a quasi-homogeneous and isotropic expansion) and an adiabatic hypothesis is as-

TABLE II Values of the material parameters of the gas and Newton fluid

Parameter	Name	Value
Viscosity of the liquid	$\eta_0$ (MPa.s)	$1 \times 10^{-3}$
Heat capacity	$\rho_{cv}$ ( $\text{J K}^{-1} \cdot \text{m}^{-3}$ )	$1.3 \times 10^3$
Heat conductivity	$k_f$ ( $\text{W K}^{-1} \text{m}^{-1}$ )	$2.63 \times 10^{-2}$
Conversion rate	$\lambda_g$ ( $\text{s}^{-1} \text{m}^{-2}$ )	$1.39 \times 10^{-2}$
Reaction exponent	$\mu_g$	1
Enthalpy of gas creation	$\delta H_g$ ( $\text{J mol}^{-1}$ )	$1 \times 10^{-4}$
Rate of moles created in the bubble	$\kappa$	10

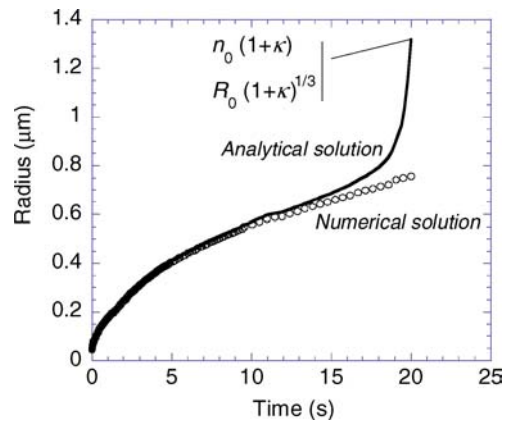


Figure 1 Evolution of the radius of a single bubble in a quasi-infinite medium during the expansion as function of time: comparison between the analytical solution and the finite element simulation.

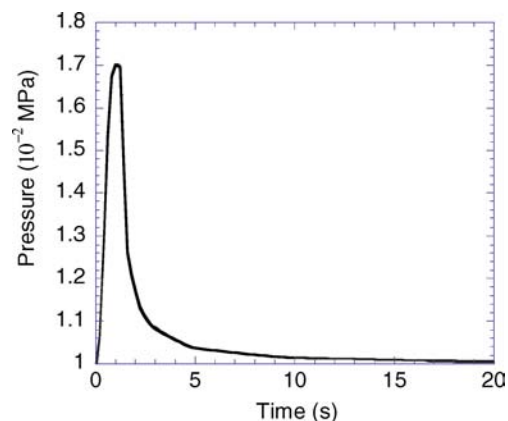


Figure 2 Evolution of the pressure in the bubble as function of time during the expansion.

sumed on them (the temperature is quasi-homogeneous in the centre of the foam). These hypotheses would not be realistic near the skin.

Initially, the pressure in the bubbles is equal to atmospheric pressure, which implies that the number of

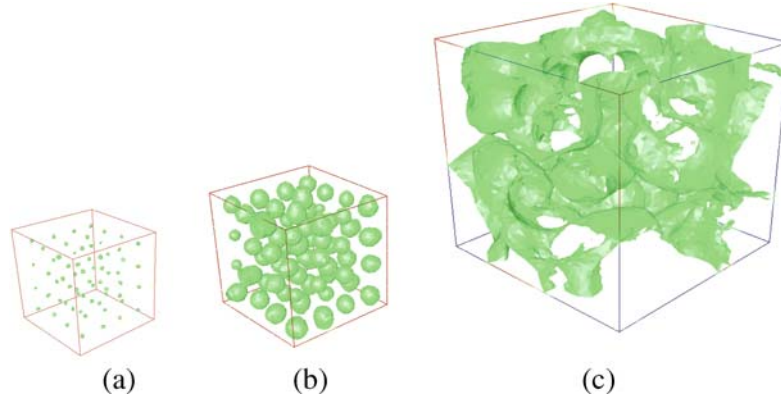


Figure 3 Evolution of foam microstructure in a cube (initial dimension  $1 \text{ mm}^3$ ) for 64 bubbles with a random initial radius distribution, after fixed times of reaction (a)  $t = 0 \text{ s}$ , initial germs, (b)  $t = 10 \text{ s}$ , beginning of expansion, (c)  $t = 60 \text{ s}$ , after coalescence.

moles they initially contain is different. Even if the chemical conversion rate is independent of the initial number of moles, this random initial distribution is sufficient to account for the heterogeneous and anisotropic final distribution of the bubbles. The matrix is assimilated to a shear-thinning fluid, whose behaviour is expressed by a Carreau-Arrhenius law:

$$\eta(\dot{\gamma}, T) = \eta_0(T_{\text{ref}}) e^{\frac{E}{R} \left( \frac{1}{T} - \frac{1}{T_{\text{ref}}} \right)} \times \left( 1 + \left( a(T_{\text{ref}}) e^{\frac{E}{R} \left( \frac{1}{T} - \frac{1}{T_{\text{ref}}} \right)} \right)^2 \dot{\gamma}^2 \right)^{\frac{m-1}{2}} \quad (9)$$

$E$  is the activation energy,  $a$  is a characteristic time and  $m$  the power-law exponent. The curing reaction affects the viscosity of the fluid by a function  $f_g$ , which follows the model developed by Castro and Macosko [18]:

$$\eta(\dot{\gamma}, T, \beta) = \eta(\dot{\gamma}, T) f_g(\beta)$$

where  $f_g(\beta) = \left( \frac{\beta_{\text{gel}} - \beta}{\beta_{\text{gel}}} \right)^{-n_g}$  (10)

$\beta_{\text{gel}}$  is the gel point and  $n_g$  a constant. The values of these new material parameters are given in Table III and are based on the results of Dimier et al. [19]. The parameters of the gas bubbles are the same as in Section 3.1.

TABLE III Values of the material parameters of the reactive system

Parameter	Name	Value
Initial viscosity of the liquid	$\eta_0$ (MPa.s)	$1 \cdot 10^{-3}$
Density	$\rho$ ( $\text{kg} \cdot \text{m}^{-3}$ )	$1 \cdot 10^3$
Characteristic time of Carreau Law	$a$ (s)	2
Power-law index	$m$	0.25
Activation energy	$E$ ( $\text{J} \cdot \text{mol}^{-1}$ )	$7.2 \cdot 10^3$
Gel point	$\beta_{\text{gel}}$ (%)	95
Gel exponent	$n_g$	1.6
Curing rate	$\lambda_p$ ( $\text{s}^{-1} \cdot \text{m}^{-2}$ )	$1.39 \cdot 10^{-2}$
First reaction exponent	$\mu_p$	0.3
Second reaction exponent	$\nu_p$	1.6

Fig. 3 presents, after fixed times of reaction, the position of the interfaces between fluid and gas bubbles, from an initial volume of liquid ( $1 \text{ mm}^3$ ) (Fig. 3a) to an expanded textured volume (Fig. 3c). During the bubbles expansion, the global volume of the mixture increases of about 360%. The growth and the coalescence of the bubbles are visible in Fig. 3c near the gel point ( $\beta \approx \beta_{\text{gel}}$ ).

The coalescence of the bubbles is heterogeneous and anisotropic. Fig. 4 shows the evolution of the volumic cell size distribution (defined as the product of the number of bubbles of a given size by their size divided by the total gas volume) in function of the radius. The main results are:

- at the beginning of the expansion, the growth of the smaller bubbles population is the fastest since the number of the greatest bubbles decreases. This corresponds to the increase of pressure up to its maximal value, due to the creation of gas moles, which favours the smallest bubbles ( $0 < t < 40 \text{ s}$ ),
- later, the density of smaller bubbles decreases ( $< 10\%$ ,  $40 < t < 60 \text{ s}$ ). This phenomenon is related to two effects: when the pressure remains constant during the expansion, it exists a critical radius, depending on the  $S_i/V_i$  ratio for each bubble, below which the expansion slows down (see Equations 7–8). Moreover, if two bubbles of small size coalesce, they disappear in the population of smallest

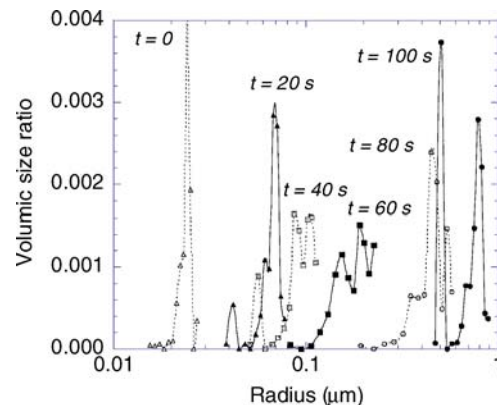


Figure 4 Evolution of the cell size distribution during the expansion (125 bubbles).

bubbles, so that the number of bubbles increases in the other populations. The greatest bubbles expand gradually due to a more important exchange surface  $S_i$  (Equation 2), leading to the development of two distributions of “middle” and “large” bubbles ( $60 \text{ s} < t < 80 \text{ s}$ ),

- finally, the “largest” bubbles continue to grow fast since the growth of the “middle size” bubbles becomes slower ( $80 < t < 100 \text{ s}$ ).

This type of expansion leads to a bimodal cell foam, in which small bubbles are trapped between larger ones.

According to these results and to the influence of the heterogeneity of bubbles in the mixture, the gas rate is plotted as function of time, for different initial numbers of bubbles (respectively 1, 8, 27, 64 and 125 bubbles). The results show that the gas rate is a variable that is not sufficient to describe the topological evolution of the foam (Fig. 5a). We have to introduce a new parameter, the number of bubbles by unit of volume in the mixture,  $N$ . This topological parameter can constitute a new variable in the model, whose evolution has to be correlated to that of the gas rate, taking into account the coalescence of the bubbles (Fig. 5b). The porosity of the foam is calculated as the ratio of the total volume of gas by the volume of the material domain.

At the difference of the radius evolution shown in Fig. 1 in the case of a single bubble in a non-reactive medium, the evolution of the viscosity of the matrix limits the expansion of the bubbles. The relative viscosity  $\eta(t)/\eta_0$  tends to infinity as the polymerization

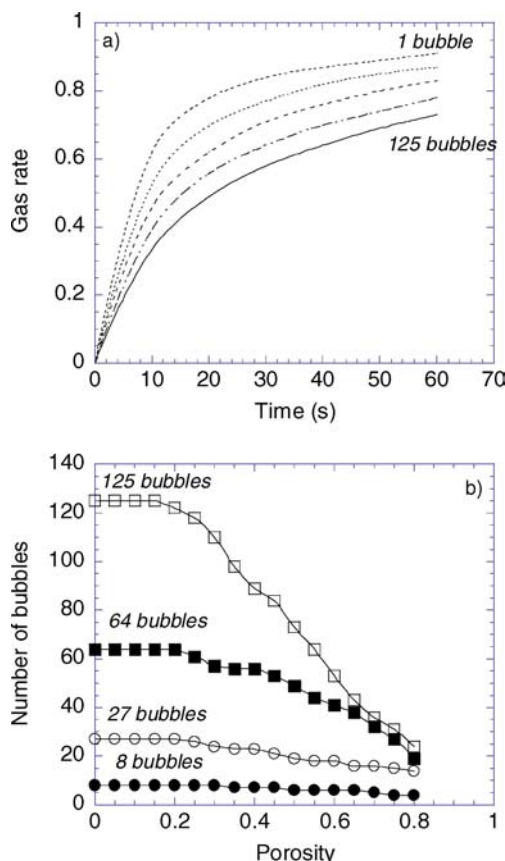


Figure 5 Characterisation of the importance of the number of bubbles per volume unit during the expansion: (a) evolution of the gas rate, (b) evolution of the number of bubbles by coalescence.

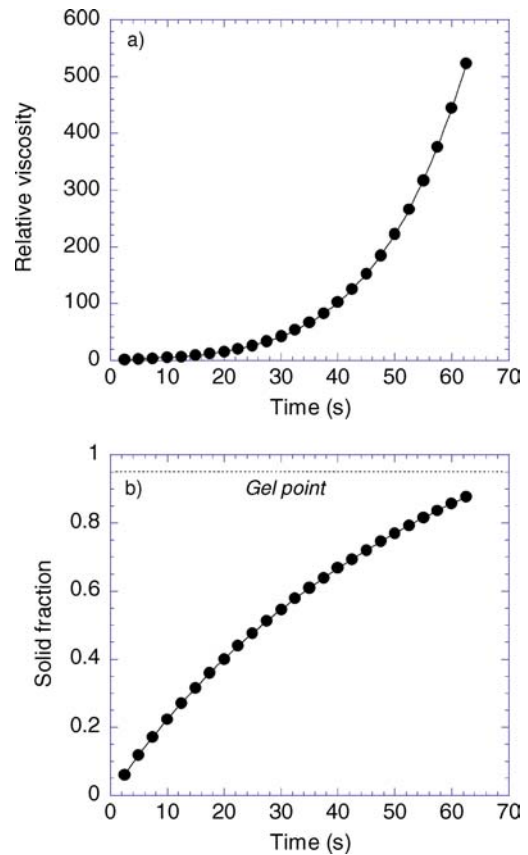


Figure 6 Evolution of the polymer properties due to the curing reaction during the expansion; (a) evolution of the relative viscosity  $f_g$ , (b) evolution of the solid polymer fraction.

rate tends to the gel point (Fig. 6a and b). At the same time, the velocity of the mixture (the velocity of the liquid in the thin walls around the bubbles) tends to zero.

### 5. Conclusion

A model describing the expansion of flexible foams during the manufacturing process has been proposed, considering the evolutions of the interface between matrix and gas bubbles at the microscopic scale. Two mechanisms have been taken into account for this evolution: the difference of pressure between the gas and the liquid due to creation of gas in the mixture, and the curing of the matrix. The germination step of the bubbles in the mixture has been described, in a first approximation, by an initial distribution of small bubbles in the mixture. Finally, a phenomenological equation has been proposed to describe the evolutionary rheological properties of the fluid during the cure. The computational domain is discretized in space-time finite elements. Flow equations are solved using mixed finite elements, whereas free surface and gas rate are determined using a finite element based V.O.F. method associated with a Space-Time Discontinuous Galerkin technique. Numerical implementation has been validated on a simple test: the expansion of a single bubble in a quasi-infinite medium. The same methodology has been then used to characterize the microstructure of a foam during the manufacturing process. According to the numerical results, some considerations on the

topology and the evolution of rheological properties have been done.

Main perspectives arising from this work concern the comparison with real observations during the process. On the other hand, the numerical modelling should taken into account the diffusion and germination mechanisms, in order to predict the phenomena appearing close to the external surface of the foam (skin effects due to cooling, percolation mechanisms [20]).

### Acknowledgements

J. Bikard was granted by the French Ministère de la Recherche, through the project CANAL–SALVE, headed by G. Della Valle and developed under the authority of INRA (Institut National de la Recherche Agronomique)

### References

1. L. LEFEBVRE and R. KEUNINGS, Mathematical Modelling and Computer Simulation of the Flow of Chemically-Reacting Polymeric Foams, in "Mathematical Modelling for Materials Processing," edited by M. Cross, J. F. T. Pittman, R. D. Wood, (Clarendon Press, Oxford, 1993) p 417.
2. G. OERTEL, in "Polyurethane Handbook" (Hanser Publishers, Munich, 1985).
3. D. WEAIRE and S. HUTZLER, "The Physics of Foams" (Oxford University Press, Oxford, 1999).
4. E. MORA, L. D. ARTAVIA and C. W. MACOSKO, Modulus development during reactive polyurethane foaming, *J. Rheol.* **35** (1991) 921.
5. S. L. EVERITT, O. G. HARLEN, H. J. WILSON and D. J. READ, Bubble dynamics in viscoelastic fluids with application to reacting and non-reacting polymer foams, *J. Non Newt. Fluid Mech.* **114** (2003) 83.
6. P. PERZYNA, Fundamental problems in viscoelasticity, *Adv Appl. Mech.* **9** (1966) 243.
7. M. AMON and D. C. DENSON, A study of the dynamics of foam growth: analysis of the growth of closely spaced spherical bubbles, *Polym. Eng. Sci.* **24** (1984) 1026.
8. M. I. ARANGUREN and R. J. J. WILLIAMS, Kinetic and statistical aspects of the formation of polyurethanes from toluene diisocyanate, *Polymer* **27** (1986) 425.
9. J. BIKARD, T. COUPEZ and B. VERGNES, Modélisation numérique multidomaines de l'expansion réactive d'une mousse polymère par création de gaz, Actes du 38ème Colloque du Groupe Français de Rhéologie, CD ROM (2003), Brest, France.
10. G. O. PILOYAN, I. D. RYABCHIKOV and O. S. NOVIKORA, Determination of activation energies of chemical reactions by differential thermal analysis, *Nature*, **5067** (1966) 1229.
11. R. B. KELLOG and B. LIU, A finite element method for the compressible Navier-Stokes equations. *SIAM J. Num. Anal.*, **33** (1996) 788.
12. D. N. ARNOLD, F. BREZZI and M. FORTIN, A stable finite element for Stokes equations. *Calcolo* **21** (1984) 344.
13. S. BATKAM, J. BRUCHON and T. COUPEZ, A space-time discontinuous Galerkin method for convection and diffusion in injection moulding. *Intern. J. Form. Proc.* **7** (2003) 11.
14. E. PICHELIN and T. COUPEZ, Finite element solution of the 3D mold filling problem for viscous incompressible fluid. *Comput. Meth. Appl. Mech. Eng.* **163** (1999) 371.
15. E. BIGOT and T. COUPEZ, Capture of 3D moving free surfaces and material interfaces by mesh deformation. in Proceedings ECCOMAS 2000, Barcelona, CD Rom (2000).
16. J. BRUCHON and T. COUPEZ, Étude 3D de la formation d'une structure de mousse polymère par simulation de l'expansion anisotherme de bulles de gaz, *Mécanique & Industries* **4** (4)(2003) pp. 331.
17. Z. H. TU, V. P. W. SHIM and C. T. LIM, Plastic deformation modes in rigid polyurethane foam under static loading, *Int. J. Solids Struct.*, **38** (2001) 9267.
18. J. M. CASTRO and C. W. MACOSKO, Kinetics and rheology of typical polyurethane reaction injection molding systems, SPE ANTEC Tech. *Papers* (1980) 434.
19. F. DIMIER, N. SBIRRAZZUOLI, B. VERGNES and M. VINCENT, Curing kinetics and chemorheological analysis of polyurethane formation, *Polym. Eng. Sci.*, **44** (2004) 518.
20. G. A. CAMPBELL, Polyurethane foam process development. A systems engineering approach. *J. Appl. Polym. Sci.* **16** (1972) 1387.

Received December 2004

and accepted April 2005